

A Pair of Lensed Galaxies at $z = 4.92$ in the Field of CL1358+62¹Marijn Franx²Garth D. Illingworth³Daniel D. Kelson³Pieter G. van Dokkum²Kim-Vy Tran³

To appear in ApJ Letters, 486, L75 (Sept 1997)

A B S T R A C T

The cluster CL1358+62 displays a prominent red arc in WFPC2 images obtained with the Hubble Space Telescope. Keck spectra of the arc show Ly emission at 7204 Å, a continuum drop blueward of the line, and several absorption lines to the red. We identify the arc as a gravitationally lensed galaxy at a redshift of $z = 4.92$. It is the highest redshift object currently known. A gravitational lens model was used to reconstruct images of the high-redshift galaxy. The reconstructed image is asymmetric, containing a bright knot and a patch of extended emission 0.04 from the knot. The effective radius of the bright knot is 0.022 or $130h_{50}^{-1}$ pc. The extended patch is partially resolved into compact regions of star formation. The reconstructed galaxy has $I_{AB} = 24$, giving a bolometric luminosity of $3 \times 10^{11} L_{\odot}$. This can be produced by a star formation rate of $36 h_{50}^{-2} M_{\odot} \text{ yr}^{-1}$ ($q_0 = 0.5$), or by an instantaneous starburst of $3 \times 10^8 M_{\odot}$. The spectral lines show velocity variations on the order of 300 km s^{-1} along the arc. The Si II line is blue shifted with respect to the Ly emission, and the Ly emission line is asymmetric with a red tail. These

¹Based on observations taken with the NASA/ESA Hubble Space Telescope obtained at the Space Telescope Science Institute, which is operated by AURA under NASA contract NAS5-26555, and observations obtained at the W. M. Keck Observatory, which is operated jointly by the University of California and the California Institute of Technology

²Kapteyn Institute, P.O. Box 800, NL-9700 AV, Groningen, The Netherlands

³University of California Observatories / Lick Observatory, Board of Studies in Astronomy and Astrophysics, University of California, Santa Cruz, CA 95064

spectral features are naturally explained by an outflow model, in which the blue side of the Ly α line has been absorbed by outflowing neutral H I. Evidence from other sources indicates that outflows are common in starburst galaxies at high and low redshift. We have discovered a companion galaxy with a radial velocity only 450 km s⁻¹ different than the arc's. The serendipitous discovery of these two galaxies suggests that systematic searches may uncover galaxies at even higher redshifts.

Subject headings: galaxies: formation | galaxies: evolution { galaxies: starburst
 { galaxies: clusters: individual (CL1358+62) | gravitational lensing

1. Introduction

The number of spectroscopically confirmed high-redshift galaxies is increasing rapidly. Steidel et al. (1996a,b) demonstrated that galaxies at redshifts $z \gtrsim 3$ can be found very efficiently by deep imaging and color selection (the U or B-band "dropout" technique). The absorption to the blue of Ly α by the Ly α forest, and by source and intergalactic H I beyond the Ly limit, are unique signatures of high-redshift objects (Madau 1995, Madau 1997). Deep searches for Ly α emitters have been less successful, but have recently resulted in detections at high redshift (e.g., Hu and Madau 1996, Djorgovski et al. 1996). Although most of the photometric searches have concentrated on galaxies at redshifts $z = 3-4$, similar searches can, in principle, be used to find even higher redshift galaxies.

Our serendipitous discovery of two galaxies at $z = 4.92$ reported here suggests that $z \gtrsim 5$ galaxies may be found by similar photometric "dropout" techniques. One of the galaxies is strongly gravitationally lensed and is detected as a very red arc in the $z = 0.33$ cluster CL1358+62. This cluster was selected for detailed study of its member galaxies using HST imaging and extensive WHT and Keck spectroscopy. An earlier search for arcs in this cluster was unsuccessful (LeFevre et al. 1994), so the presence of the arc in the HST image was unexpected. HST and Keck are able to exploit the magnification provided by the cluster lens to provide spectroscopic observations of a high redshift galaxy at unprecedented spatial resolution.

2. Observations

We obtained a large mosaic of multicolor WFC2 images of the cluster for a detailed study of the cluster members. The integration time was 3600 s in each of the F606W ("R")

and F814W (I') filters. The data have been described in Kelson et al. (1997) and van Dokkum et al. (1997). A color image of the central part of the cluster is shown in Figure 1 (Plate 1). Several arcs can be seen, of which the long red arc (B-C) is the brightest, lying $21''$ from the central CD galaxy. This arc is distorted by the bright elliptical galaxy north of component B. An additional faint lensed component D is located still further north. The arc is strikingly knotty, with both tangential and radial structure.

The symmetric distribution of the knots suggest that we are seeing a fold arc. We therefore searched for the expected counterimage. We identified a candidate counterimage $29''$ east of the CD galaxy, marked A in Figure 1. The colors of the arc and the counterimage are consistent.

Spectra of the arc and the counterimage were obtained at the W. M. Keck Telescope in 1996 May, June, and 1997 February. The best spectrum was taken with a long-slit in February, using the Low Resolution Imaging Spectrograph (LRIS). For this LRIS spectrum, the slit was aligned with the arc (B-C), and a resolution of 4.3 \AA FWHM was attained. The spectrum is shown in Figure 2 (Plate 2). The dominant features are the emission line at 7204 \AA and the continuum drop to the blue side of this emission line. The continuum disappears further in the blue. The spectrum varies along the arc (e.g., the continuum is enhanced in the bright knot and the ratio of Ly α to continuum changes).

Figure 3 is a spatially-averaged spectrum showing the emission line and continuum step at 7204 \AA and absorption lines to the red. We mark the absorption line features found by Lowenthal et al. (1997) in an average of 12 high redshift galaxies. Each absorption line can be identified in the arc spectrum. These spectral features provide a secure redshift for the source galaxy ($z = 4.92$) and allow us to identify the emission feature as Ly α . The redshift of $z = 4.92$ is currently the highest spectroscopically measured for a galaxy or active nucleus. The narrow Ly α emission, the absence of other emission lines, and the broad spatial extent imply that the continuum is stellar.

The spectrum suggests that the continuum break across Ly α is about a factor of 1.9. This is an underestimate, as the break is very likely diluted by a weak contribution from the bright cluster galaxy. This galaxy contributes a flux in the I band similar to that of the arc. The broad band colors, and the spectrum of the bright knot at the end of the arc suggest that the true flux ratio across the break is a factor of 3 or more.

We also obtained spectra of the candidate counterimage in multislit mode. It was found to have an emission line at the same redshift as the arc (Figure 4b), confirming its status as a counterimage of the arc. In what follows, we refer to the galaxy that is gravitationally lensed into these arcs as G1. To our surprise, we found an unexpected emission line from a

faint, red, galaxy (G 2) that lies 37° W of the arc (Figure 4c). It was observed by chance through a slitlet pointed at another galaxy. It has the same shape and width as the Ly emission from the arc. Both Ly lines have a tail to the red, and a steep cutoff in the blue. This signature has been found previously in two nearby starburst galaxies (Lequeux et al. 1995, Kunth et al. 1996). As these authors show, this asymmetry is caused by an outflow. Our results indicate that high resolution spectra can be used to distinguish between Ly emission and O [II] 3727 Å: at high resolution O [II] is resolved into a symmetric doublet, without the asymmetry displayed by Ly (Figure 4).

The wavelength peaks of the lines in object G 2 and the arcs are very similar: we measure a wavelength of 7193 Å for G 2, versus 7204 Å for the arcs. Object G 2 has a magnitude of $I_{814,AB} = 25.1$, and is also very red (see Figure 1, Plate 1). Thus the emission is highly likely to be Ly, and G 2 is at $z = 4.92$. After correction for lensing (see below), the projected distance between G 2 and G 1 is $200 h_{50}^{-1}$ kpc, and the velocity difference is 450 km s^{-1} (with an unknown error dominated by the outflow in both galaxies).

3. Analysis

The imaging and spectroscopy leave little doubt that we have found a multiply-imaged, distant galaxy. We have been able to reproduce the geometry of the arcs by modeling the cluster as an isothermal potential. An additional isothermal potential was added to model the effect of the elliptical galaxy north of the arc. The general form of the model is shown in Figure 5 (Plate 3). This model successfully reproduces the fold arc and the counterarc. Furthermore, the model produces only one counterimage, because the source lies outside the radial caustic. The Einstein radius of this model is $21^{\prime\prime}$. For an isothermal model, this implies a velocity dispersion of 970 (990) km s^{-1} for $q_p = 0.5$ (0.05), which is similar to the observed dispersion of 1080 km s^{-1} for the galaxies (Fisher et al., in preparation).

We use this lens model to reconstruct the intensity distribution of the source galaxy, G 1. The two parts of the fold arc, and the counterimage were reconstructed separately. The reconstructions are shown in Figure 1 with the color information and with higher contrast in Figure 5 (Plates 1 and 3). The resolution varies from one reconstruction to the next, but is particularly high for the west part of the fold arc where the magnification is large ($5 - 11$). The morphology is a strong function of the resolution. At the lowest resolution (with $0.05 - 0.1$ pixels in the source plane), the galaxy appears to consist of a bright knot and a diffuse extended structure. These features contribute roughly equally to the total flux. At the highest resolution, half of the flux of the extended structure is resolved into small knots. The bright knot is very small. It is extended in a PC image, but this is partly

due to the PC point spread function. After deconvolution and reconstruction, we find that the half-light radius of the knot is 22 milliarcseconds or $130h_{50}^{-1}$ pc ($q_b = 0.5$).

Nearby starburst galaxies show comparable irregular morphologies in the UV (Meurer et al. 1995) with dense knots of star formation. Meurer et al. refer to these knots as "super-star clusters" and suggest that they are possibly the progenitors of globular clusters. The dense knots can contribute between 20 to 50% of the UV flux. The bright knot in G 1 is much more luminous than those in nearby starburst systems, but otherwise the similarity is striking.

3.1. Star Formation at $z = 5$

The lens model implies that the unlensed magnitudes of G 1 and G 2 are $I_{814,AB} = 24$ and 25.4, respectively. The corresponding star formation rates (SFR) are 36 and 9 M_{\odot}/yr ($q_b = 0.5$). This is based on model predictions by Bruzual and Charlot (1993) for a stellar population with continuous star formation at an age of 10^8 years, and a Salpeter IMF. An instantaneous burst model requires a minimum mass of $3 \times 10^8 M_{\odot}$. If dust is present, the above SFRs would increase, possibly substantially (Meurer et al. 1997). Even so, the inferred star formation rate is very high. Over a period of 10^8 years, which is only 1/6 of the Hubble time at $z = 4.92$, 20-40% of the mass of the Galactic bulge can be formed.

Meurer et al. (1995, 1997) suggest that there is a natural upper limit to the surface brightness of starbursts. We find that the mean surface brightness of G 1 is low at $1.4 \times 10^{10} L/\text{kpc}^2$. However, the surface brightness of the knot in G 1 is much higher, at $3 \times 10^{12} L/\text{kpc}^2$. This is significantly higher than the 90th percentile upper limit of $2 \times 10^{11} L/\text{kpc}^2$ derived by Meurer et al. (1997), although it is close to the highest value in their sample. The bright knot in G 1 may appear extreme because it is unique amongst high redshift galaxies in being mapped with very high spatial resolution (from the magnification provided by the cluster lens). At the usual WFC2 resolution, the knot in G 1 is undersampled. This undersampling may pose a problem for size estimates based on WFC2 observations of unlensed high redshift galaxies.

The bright knot in G 1 is too massive to evolve into a typical globular cluster. If the knot remains bound, it is more likely to end up in the nucleus of the galaxy, and it is possibly one of the progenitors of the bulge. A dynamical mass estimate of the knot would be valuable.

3.2. Velocities and Spatial Structure in the Spectrum

The arc is the first high redshift galaxy for which it is possible to obtain spatially-resolved spectral information (Figure 6). The peak of the Ly α emission varies by about 7 Å. This variation is real, and is larger than expected from positional variations of the knots on the slit. The Si II 1260 Å is blue shifted with respect to the Ly α peak by 300 km s^{-1} , and the velocity variation is on the order of 300 km s^{-1} . The width of the Si II line is approximately constant at 12 Å (or 2 Å in the rest frame), which is equivalent to a velocity dispersion of 200 km s^{-1} . However, these velocities should not be interpreted as indicative of the gravitational potential of G 1.

The blue shifted Si II absorption, and the asymmetric Ly α emission are naturally explained by an outflow model. Outflowing neutral and ionized material accounts for the Si II absorption, and absorbs the blue part of the Ly α emission line. The low continuum blueward of Ly α (Fig. 2) is consistent with the presence of a significant, blueshifted H I column. G 1 is thus similar to M 33, a nearby starburst galaxy. Lequeux et al. (1995) observed the same blueshifted interstellar absorption lines and asymmetric Ly α profile in M 33. They verified that the interstellar absorption lines were blueshifted with respect to the bulk of the galaxy. Another such case was presented by Kunth et al. (1996). Furthermore, Heckman and Leitherer (1997) found unambiguous evidence that UV absorption lines in NGC 1705 are produced by outflowing material. In general, outflows are present in most luminous starbursts at low redshifts (e.g., Heckman, Armus, and Miley 1990).

Outflows may also be the norm for high redshift galaxies: G 2 has the same asymmetric Ly α profile, and the Ly α emitter found by Djorgovski et al. (1996) has a red tail. Furthermore, the average spectrum of 12 high redshift galaxies obtained by Lowenthal et al. (1997) shows a velocity offset between the Ly α emission, and the Si II absorption. Trager et al. (1997) found a similar blueshift for two galaxies at $z = 4$.

The Ly α emission may also be redshifted with respect to the system velocity because of absorption by the Ly forest. This does not appear to be the dominant effect for the arc, as the high resolution spectrum in Figure 4a shows a very strong drop in the blue. Furthermore, the blue edge of the line shows velocity variations across the slit. The case is less clear for other high redshift galaxies where the spectra are typically at lower resolution.

The apparent ubiquity of outflows in galaxies with substantial SFRs, casts doubt on the suggestion by Steidel et al. (1996a) that the regular rotation caused the broadening of the interstellar absorption lines in high redshift galaxies. This is unfortunate since it would be very useful to find a method of measuring the mass of high redshift galaxies. The

large width (200 km s^{-1}) of the Si II line towards the bright knot in the galaxy is another argument against a rotational origin for the observed motions. It is hard to reconcile a systematic velocity variation of this magnitude across the knot with the small size of the knot. The velocity variations in the Ly α and Si II across the arc are probably due to differences in the outflow velocity and absorption column density. The bottom line is that wavelength gradients in Ly α or the interstellar absorption lines cannot be used to infer reliably the mass of such star-forming galaxies.

4. Conclusions

We have discovered a red arc and a counterimage of a distant galaxy that is gravitationally lensed by the cluster CL1358+62 at $z = 0.33$. The lensed galaxy and a second companion galaxy have secure redshifts of $z = 4.92$. The arc has an irregular structure, and image reconstructions show that most of the flux comes from very small knots. The morphology of the reconstructed galaxy is very similar to that of nearby starburst galaxies in the UV (Meurer et al. 1995), which are also very irregular with dense star-forming knots. The surface brightness of the brightest knot in the lensed galaxy is higher than the 90th percentile upper limit derived by Meurer et al. (1997) for nearby and distant starbursts. The mass and size of this bright knot suggest that it might be a "bulge-building" subclump. It remains to be seen whether this lensed galaxy (G1) is typical of the population of starbursting galaxies at $z \sim 5$.

The irregular structure of G1 can be contrasted with the $z = 3$ galaxies studied by Gavrilis et al. (1996). These authors found that many of those galaxies are compact with little substructure. The high redshift galaxies in the Hubble Deep Field are more similar to our reconstructed images of G1 (e.g., Lowenthal et al. 1997, Steidel et al. 1996b). The morphology of G1 is a strong function of resolution: at the lowest resolution, half of the flux appears to originate from a smooth, extended component. Half the flux of this component is resolved into knots at the highest resolution. Other high redshift galaxies might display similar irregular morphologies if they were to be imaged at much higher resolution.

Our results, and the data presented by others, indicate that radial outflows dominate the kinematics of the absorption line gas in high redshift galaxies. These radial outflows are a general feature of luminous starburst galaxies in the nearby universe. Radial outflows of hundreds of km s^{-1} can quickly disperse the reservoir of gas from which the stars formed. The rest-UV appearance of these galaxies is likely to be dominated by short-lived areas of intense star formation. IR observations are needed to characterize the overall morphology, since the UV structure will not be representative of the distribution of older stars in these

galaxies.

Our serendipitous discovery of the two galaxies at $z = 4.92$ raises the question of the surface density of such objects. Their unlensed $I_{814,AB}$ magnitudes are estimated to be 24 and 25.4. The results by Lanzetta et al. (1996) suggest an upper limit of $z > 4$ galaxies of 0.4 arcmin^{-2} for $I_{814,AB} < 26$. Madau et al. (1996) found B drop-out candidates in the Hubble Deep Field with $I_{814,AB}$ magnitudes of 26 or higher. The $I_{606,AB} - I_{814,AB}$ color of the arc is in good agreement with the models of high redshift starbursts (Madau et al. 1996), which indicates that candidates might be found by shifting the drop-out techniques further into the red. Finding such objects with emission line searches may be more difficult. While the unlensed Ly α flux of the arc is comparable to the fluxes for the Ly α selected galaxies found by Hu and McMahon (1996), it is comparable to the rms noise in the deep field searches for Ly α (e.g., Thompson, Djorgovski, and Trauger, 1995).

We thank Dan Fabricant and Tim Heckman for their comments on the manuscript. We appreciate the valuable comments of an anonymous referee. The assistance of those at STScI who helped with the acquisition of the HST data is gratefully acknowledged. We also appreciate the effort of those who developed the Keck telescopes and the LRIS spectrograph, and those who supported our efforts at Keck. Support from STScI grants G O 05989.01-94A, G O 05991.01-94A, and A R 05798.01-94A is gratefully acknowledged.

REFERENCES

- BruzualA., G. & Charlot, S. 1993 *ApJ*, 405, 538
- Djorgovski, S. G., Pahre, M. A., Bechtold, J., Elston, R., 1996, *Nature*, 382, 234
- Gialalisco, M., Steidel, C. C., & Mochetto, D. 1996, *ApJ*, 470, 189
- Heckman, T. M., Amus, L., & Miley, G. K., 1990, *ApJS*, 74, 833
- Heckman, T. M., & Leitherer, C. 1997, *AJ*, submitted
- Hu, E. M. & McMahon, R. G., 1996, *Nature*, 392, 231
- Kelson, D., van Dokkum, P. G., Franx, M., Illingworth, G. D., Fabricant, D., 1997, *ApJ*, 478, L13
- Kunth, D., Lequeux, J., MasHesse, J. M., Terlevich, E., & Terlevitch, R., 1996, preprint, astro-ph/9612043

- Lanzetta, K. M., Yahil, A., & Fernandez-Soto, A. 1996, *Nature*, 381, 759
- Le Fevre, O., Hammer, F., Angonin, M. C., Gioia, I. M., Luppino, G. A., 1994, *ApJ*, 422, L5.
- Lequeux, J., Kunth, D., Mas-Hesse, J. M., & Sargent, W. L. W. 1995, *A & A*, 301, 18
- Lowenthal, J. D., et al., 1997, *ApJ*, 481, 673
- Madau, P. 1995, *ApJ*, 441, 18
- Madau, P., Ferguson, H. C., Dickinson, M. E., Gialalisco, M., Steidel, C. C., Fruchter, A. 1996, *MNRAS*, 283, 1388
- McMahon, R. G., 1997, in *The Early Universe with the VLT*, ed. J. Bergeron, Springer Verlag, Berlin, p333
- Meurer, G. R., Heckman, T. M., Leitherer, C., Kinney, A., Robert, C., Garnett, D. R., 1995, *AJ*, 110, 2665
- Meurer, G. R., Heckman, T. M., Lehnert, M. D., Leitherer, C., Lowenthal, J., 1997, *AJ*, accepted, astro-ph/9704077
- Steidel, C. C., Gialalisco, M., Pettini, M., Dickinson, M., & Adelberger, K. L. 1996a, *ApJ*, 462, 17L
- Steidel, C. C., Gialalisco, M., Dickinson, M., & Adelberger, K. L. 1996b, *AJ*, 112, 352
- Thompson D., Djorgovski, S., Trauger, J. 1995, *AJ* 110, 963
- Trauger, S. C., Faber, S. M., Dressler, A., & Oemler, A. Jr. 1997, *ApJ*, 485, 92
- van Dokkum, P. G., Kelson, D., Franx, M., Illingworth, G. D., Fabricant, D., 1997, in preparation.

Figures 1,2,5 in jpeg format. For high quality images see
<http://www.astro.rug.nl/~franx/papers/arc> or <ftp://www.astro.rug.nl/preprint/238.ps.gz>

Fig. 1. | [Plate 1] HST image of the center of the cluster CL1358+62 at $z = 0.33$. The cluster was imaged in the F606W and F814W passbands. The red arc is conspicuous, and is marked B and C. Other images of the lensed galaxy at $z = 4.92$ are marked (A and D). The reconstructions of the images A-C are displayed at the bottom at a highly expanded scale. These images may be compared with the lens geometry and lens models shown in Fig. 4 (Plate 3). The bright knot is unresolved in the WF reconstruction of C, and only marginally resolved in the reconstructed PC image shown to the right. The inset at the upper right displays at enhanced contrast a second galaxy, G2, that was found serendipitously $37''$ west of the arc.

Fig. 2. | [Plate 2] The best Keck spectrum of the red arc is displayed at the top. The spectrum is dominated by the emission line at 7200 \AA , which we identify as Ly γ . The bright knot in the arc is visible in the lower part of the arc spectrum. The distance from the brightest knot is indicated along the vertical axis. The Si II absorption line at 1260 \AA can be identified at the red end of the spectrum. The two bottom panels show the expanded region around Ly γ and Si II. Sky lines redward of Ly γ introduce additional noise in the spectra, and are indicated by \square . The Ly γ emission varies significantly along the arc. The equivalent width of Ly γ is 21 \AA near the middle of the arc, but is low at 7 \AA at the bright knot. The continuum of the knot is strongly absorbed blueward of Ly γ , but less so for the arc as a whole. Due to the strong curvature of the arc, the bright knot at the east side of the arc was not included in the spectrum.

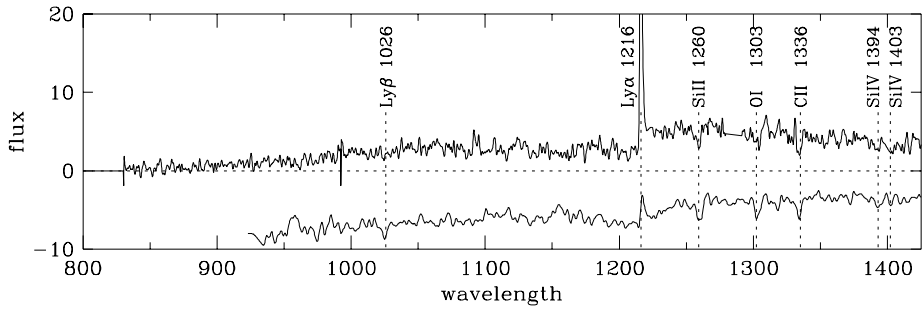


Figure 3 - Franx et al

Fig. 3. | The averaged spectrum of the arc. The Ly emission line, and the discontinuity across the emission line are clearly visible. For comparison, the average spectrum of 12 galaxies at $z = 3$ (Lowenthal et al. 1997) is shown at the bottom. All conspicuous interstellar absorption features in this average spectrum are marked, and can be identified in the spectrum of the arc. These confirm that the arc has a redshift of 4.92. The continuum has a weak contribution from the nearby elliptical galaxy, which dilutes the lines somewhat.

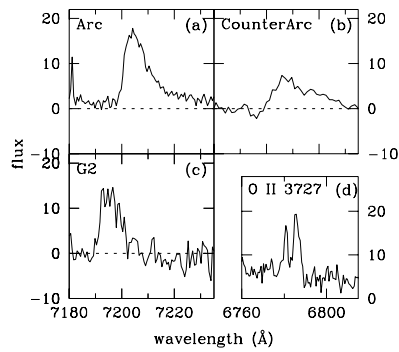


Figure 4 - Franx et al

Fig. 4. | The Ly emission lines for the arc, the counterarc, and galaxy G2. The arc and the counterarc have the same redshift. The emission line of G2 has a similar red tail and

width, strongly suggesting that the emission line is also Ly α . Panel d) shows O [III] 3727 Å emission from a field galaxy at the same spectral resolution. The 3727 Å emission is clearly resolved into a doublet, and cannot be mistaken for Ly α .

Fig. 5. | Plate 3] The lens model is shown at the top. The multiple images of the lensed galaxy are indicated. The galaxy was assigned three different levels of intensity. These are mapped into the image plane. The black curves indicate the critical lines in the image plane. The light curves indicate the caustics in the source plane. The source is indicated by G1. The middle row shows the reconstructions of images A-C at high contrast. The resolution varies greatly, and is best in the direction of greatest magnification. It is generally the highest in reconstruction C. The differences in resolution cause the apparent difference in morphology. Image A appears to consist of a bright knot, and extended emission to the south. This extended emission is resolved into knots in image C. The brightest of these knots is also visible in image B. The bottom row shows the same reconstructions after smoothing with the typical WFC2 resolution. Most of the differences between the reconstructions have disappeared.

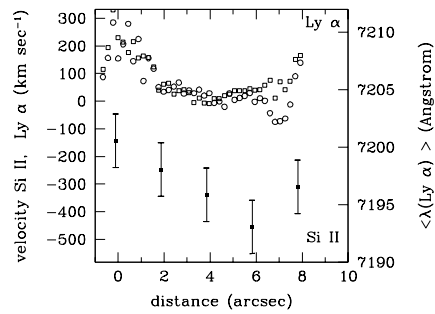


Figure 6 - Franx et al

Fig. 6. The velocity variations across the arc in the Ly α emission line and Si II 1260 \AA absorption line. The open squares and circles indicate Ly α taken with two long slit exposures. The closed squares are Si II. The features show velocity variations on the order of 300 km s^{-1} . The Si II line is systematically blueshifted with regards to the Ly α emission. The gas kinematics are most likely dominated by an outflow, which absorbs the blue Ly α emission and causes the blue shifted Si II absorption.

This figure "figure1.jpg" is available in "jpg" format from:

<http://arxiv.org/ps/astro-ph/9704090v3>

This figure "figure2.jpg" is available in "jpg" format from:

<http://arxiv.org/ps/astro-ph/9704090v3>

This figure "figure5.jpg" is available in "jpg" format from:

<http://arxiv.org/ps/astro-ph/9704090v3>